

LOG EVALUATION OF COMPACTED SHALY SANDS
OF THE MESAVERDE GROUP, UINTA BASIN, UTAH

by

G.C. Kukal
CER Corporation
P.O. Box 15090, Las Vegas, Nevada 89114

ABSTRACT

The Gas Producing Enterprises/DOE MHF demonstrations in the Uinta Basin, Utah, constitute an important part of the FY 78 Western Gas Sands Project. Extensive coring and logging of CIGE 21-15-10-22, a Mesaverde test in the Bitter Creek Field, has provided a multitude of formation evaluation data.

This paper analyzes log quality problems in the Mesaverde. Crossplot techniques are used to establish log validity, evaluate formation log parameters, and to provide methods for data normalization. Specific recommendations are made to improve the reliability of Mesaverde log evaluations.

INTRODUCTION

The Mesaverde Group of Upper Cretaceous Age is a unit of large areal extent and great thickness. It has vast, largely unproven, resources in the Uinta Basin in northeast Utah, the Piceance Basin and Sand Wash Basin in northwest Colorado, and the Green River Basin, Washakie Basin, and Red Desert Basin in southwest Wyoming. Because of the magnitude of proven and speculative reserves, the study of this marginal to subeconomic unit has become of major interest.

An important objective of DOE's Western Gas Sands Project (WGSP) is to provide effective reservoir evaluation so that completion and stimulation experiments can be adequately evaluated. By implementing the program with a combination of logging, coring, testing, and production data, it is hoped that a data base will be available so that evaluations can be made from downhole geophysical logs alone.

The Uinta Basin (Figure 1) serves as a good study area for Mesaverde resource development. The Mesaverde has already seen some marginally economic development by industry in the stratigraphic plays along the relatively shallow southeast perimeter of the basin. As part of the WGSP, DOE entered into a contract with Gas Producing Enterprises to conduct an MHF demonstration in the Natural Buttes area of the Uinta Basin. DOE financed a comprehensive coring, logging, and testing program on CIGE 21-15-10-22, Bitter Creek Field. This included complete log suites provided by two service companies. CER Corp., as consultant to the WGSP Manager, has been involved with the interpretation of these logs in an attempt to develop an interpretation model for the Mesaverde and for tight gas sands in general.

Uinta Basin Mesaverde Geology

The Uinta Basin is bounded on the north by the east-west trending Uinta Mountain Uplift, on the west by the Wasatch Uplift, on the southwest by the San Rafael Swell, and on the southeast by the Uncompahgre Uplift. It is separated from the Piceance Basin by the Douglas Creek Arch. The basin is highly asymmetrical in the north-south direction with steep dips coming off the Uinta Uplift.

The Uinta Basin has received over 30,000 feet of sediments, the bulk of which were deposited during Upper Cretaceous, Paleocene, and Eocene time. The Mesaverde Group (Upper Cretaceous) is mostly of fluvial origin and overlies marine sands and shales of the Mancos Shale.

Mesaverde Sands pinch out laterally as they were bound by the ancient braided sediment-choked stream channel. They pinch out longitudinally in response to the turbulent flow regime and resultant pool-riffle-point bar migration. The fluvial permeability pinchouts form lenticularly shaped sand beds which tend to entrap natural gas.

These lenticular sands tend to have poor reservoir characteristics. Sands are very fine-grained and at the time of deposition, tended to be interbedded and admixed with detrital clays. The detrital clays were dominantly illite and mixed layer illite-montmorillonite. As uplift proceeded during the Paleocene and Eocene and the thousands of feet of fluvial and lacustrine sediments were received by the basin, compaction and diagenesis had extreme influence on the reservoir character of the rock. Porosity and permeability were greatly diminished by the precipitation of calcium, iron, and magnesium carbonates. The detrital clays were recrystallized to authigenic illite, biotite was further altered to chlorite, and there was incipient deposition of kaolinite. The illite and chlorite tended to have a profound effect upon permeability as pore throats became lined and bridged.

Resistivity Petrophysics

Formation resistivities reflect a moderately saline formation water. R_w 's as measured from produced water from the Natural Buttes Unit, tend to maintain a fairly constant .15 ohm-m at formation temperature.

The upward migration of fluids during the compaction process undoubtedly concentrated the ions to levels higher than the depositional water, and served to make the R_w 's more uniform in vertical profile.

Drilling procedures in the Natural Buttes unit call for salt-base mud systems. This is due to imbibition by the Wasatch expandable layer clays upon prolonged contact with fresher waters, and resulting hole problems.

This unfortunate circumstance taxes resistivity logging technology to its limit. With laterolog systems, elaborate focusing electrode arrangements must be relied upon to minimize the tendency for currents to travel through the highly conductive mud column. The R_t 's become less reliable and more highly dependent upon geometric tool response. Invasion tends to exert strong influence in permeable zones due to the low porosity and deep invasion profile.

Due to the unfavorable logging conditions, R_t measurement has been one of the major evaluation problems in the Mesaverde. The availability of two sets of resistivity data from two service companies logging CIGE 21 illustrates the problem. Figure 2 compares the resistivity distributions in sandstones having greater than 4% porosity. This cumulative distribution shows a trend for Company A data to be distributed over a higher range than from Company B data. Lower resistivities (higher conductivities) are in relatively close agreement, however, ΔR_t increases exponentially as R_t increases.

R_t measurement becomes further complicated by the presence of clays. In addition to increasing tortuosity of current paths, the clay, by virtue of its structure, creates a net negatively charged crystal surface which tends to attract cations and dipolar water molecules. The environment of the clay surface is therefore one of increased conductivity compared to dilutely concentrated "bulk" water. This classical double layer then serves as a dielectric current path that supposedly conducts independently of the bulk water, resulting in a theoretical parallel circuitry within the fluid.

The ability of the "structured" water to conduct current is largely a function of clay cation exchange capacity. The tendency of the clay to remain stoichiometric becomes relaxed when subjected to an electric field. Weakly held cations overcome the poorly directed coulombic forces in response to this field and tend to migrate toward negative electrodes. When the electric field is removed, an equilibrium state is once again achieved.

Recent laboratory measurements by Schufle, Huang, and Drost-Hansen (1976) have suggested the R_t petrophysics are even more complicated than previously suspected. They present a model of vicinal (structured) water adjacent to the double layer. The long range structuring is an equilibrium condition resultant from interactions of the water molecules (H-bonds). The structuring evidently originates at the clay surface and is propagated outward across the double layer some hundreds of molecules in thickness until ordering becomes insignificant. The consequence of the vicinal layer is a decrease of viscosity, and therefore, a decrease in resistivity.

The concept of viscosity influencing resistivity is not new to log analysis. When copper wires are heated, increased atomic motion causes the wire to have increased resistance. When an electrolyte is heated, water molecules and ions also increase their motion. However, due to decreases in viscosity, the net effect is one of decreasing resistance.

Our model thus becomes one of three types of water, each supposedly conducting current independent of the others. The consequence of the vicinal layer becomes striking when bulk water decreases in volume, i.e., when pores become restricted. In the Mesaverde where pores are tens of microns in diameter, and the pores are lined by clays, the volume of the vicinal layer may even exceed bulk water volume. The effects of hydrocarbons on this model are unknown. We can postulate that hydrocarbon influence will be in interrupting the vicinal layer, reducing the vicinal to bulk water ratio and increasing the resistivity of the water-base fluid fraction. Also, of course, the hydrocarbon has the effect of increasing tortuosity of current paths, thereby increasing formation resistivity.

Density Logging

In the Mesaverde, the density log is the best quantitative porosity tool. This is because lithology remains fairly constant throughout the 2,000 to 3,000 foot section. The solid fraction of the rock is composed predominantly of quartz, which has a grain density of 2.65. Mesaverde clays average between 2.7 and 2.8 grain density. The high density clays along with minor carbonates increase the average grain density to 2.68. This seems to work very well in porosity calculations and is in good agreement with core data.

The density tool tends to have greater depth of investigation in low porosity sands. Nevertheless, the bulk of the measurement is within the radius of the invasion front. The low volume of residual gas remaining in the invaded zone when averaged with salty filtrate results in a fluid which approximates 1.0 in density.

Two sets of density data are available from CIGE 21. Availability of two density logs, run on the same well by two companies, allows log quality evaluation. Figure 3 is a histogram of Mesaverde sand density porosity for all beds having greater than 4% porosity. It shows a tendency for higher than expected porosity distribution of Company A data. Company B data has therefore been heavily relied upon in this study. Figure 4 is a "type" Mesaverde log illustrating what should be considered typical Mesaverde data. In these shaly sands, density porosity should normally be distributed over a range varying between -2% and 12-13%, using a grain density of 2.68 and a fluid density of 1.0.

The differences between the two density logs should not be considered to be the usual case. Using proper technique and calibration care, both logs should read the same. Comparison of the Company A density log with sonic response and the Company B density log suggests that the Company A density

is not constant in its calibration throughout the logged interval. That is, it is possible that there was some attempt at "downhole data normalization" during the course of the log. Company A density tends to have very close agreement with sonic and Company B density in the Castlegate but averages 1-1/2 to 3% greater porosity uphole.

The low porosities of tight gas sands create inherent problems for accurate porosity determination. Since photon intensity at the counters is inversely related to bulk density, the count rates decrease as porosity decreases. The lower count rates create a statistics problem and make it desirable to dwell in the zone longer to insure more valid measurement. Company A measurements were recorded at logging speeds approximating 1,800 feet/hour, whereas the Company B speeds were 1,200 feet/hour. The slower rate resulted in much better repeatability and bed definition.

It is unfortunate that service company standard operational procedures allow for density logging speeds of 1,800 feet/hour. While this may be adequate for thick high porosity zones, it is not good practice in the Mesaverde. Since bulk density in tight sands approaches grain density, very slight measurement errors in bulk density will create large percentage errors in porosity calculation. It is, therefore, necessary that greater care be taken in calibrating the computer to the instrument response before beginning the survey. It is desirable to monitor tool response to the calibration blocks with digital counters over sufficiently long intervals to improve statistics. In the event that digital equipment is not available, a good alternative is to photographically record the tool logging response and computer calibration for each calibration block over a two or three minute time interval. Timing marks should be recorded on the film and the time constant should allow normal logging statistics to be expressed.

It has been observed that problems sometimes arise from having neutron sources too close to the density instrument during calibration. The gamma rays emitted from these sources tend to increase the count rates of both near and far detectors creating inaccurate detector ratios and a miscalibrated log. This problem is also noticeable on the background radiation level of the gamma ray calibration. It is therefore good procedure to increase the distance separating the density tool from the neutron storage pig.

Care should also be taken that the density tool be clear of rig equipment of great mass above the plane of the catwalk. Frequently the tool is placed near the deadman at the end of the catwalk or near drill collars or drill pipe lying in the V-door. These sometimes result in erroneous tool response and a miscalibrated log.

Shaliness Determination

The resistivity discussion mentioned the importance of volume of clay. The best technique for estimating this volume and its influence upon resistivity is x-ray diffraction analysis and laboratory measurement of

cation exchange capacity. Since cores are not normally available, it becomes desirable to relate the lithological data from a few wells to more generally available log data.

Some computer interpretation systems crossplot density porosity, compensated neutron porosity and water saturation to arrive at volume of shale. Density-sonic comparisons, SP, and resistivity may also be useful. A study of these techniques as applied to tight gas sands, would be an excellent area for research and is beyond the scope of this paper.

Natural gamma radiation is a good clay indicator when uranium and thorium levels are insignificant and when clay mineral compositions remain constant over long intervals. The predominance of illite and spectral gamma ray interpretation suggest that this is generally true in the Uinta Mesaverde. Since the CIGE 21 core data is not yet available, and the best method for determination of V_{sh} is debatable, gamma ray index has been relied upon in the water saturation interpretation which follows.

Water Saturation Interpretation

The cornerstone of log analysis is the Archie Equation.

Equation 1:

$$R_t = \frac{aR_w}{\phi^m S_w^n}$$

Equation 2:

$$S_w^n = \frac{aR_w}{\phi^m R_t}$$

This expression relates water saturation to formation water resistivity, porosity, and formation resistivity. Resistivity of formation water is measured from produced water. R_t and porosity are interpreted from log measurements. The exponents "n," "m," and "a" coefficient are generally taken as "worldwide averages," 2, 2, and .8.

Using an R_w of .15, Company B density porosity, and both Company A and Company B resistivity, the Archie Equation is used to solve for water saturation. The distributions of the CIGE 21 water saturations have resulted from consistently low R_t . Company A resistivities result in lower but still unrealistic water saturations.

Many zones calculating over 100% S_w tell us that our data are wrong, our assumptions are wrong, or our equation does not take important things into consideration.

The total Shale Relation is used by
calculate S_w .

computer analysis to

Equation 3:

$$\frac{1}{R_t} = \frac{\phi^2 S_w^2}{.80 R_w (1 - V_{sh})} + \frac{V_{sh} S_w}{R_{sh}}$$

This equation is in accord with the dual water model as presented by Waxman and Smits (1968). It allows for shaliness corrections to R_t and supposes that measured resistance of solutions in capillaries is the sum of two parallel resistances; one conductance is that of bulk water, and the other is surface conductivity. The equation uses "n," "m," and "a" values of 2, 2, and .80. By solving a quadratic equation we express the relation in terms of S_w .

Equation 4:

$$S_w = \frac{0.4 R_w (1 - V_{sh})}{\phi^2} \left\{ \sqrt{\left(\frac{V_{sh}}{R_{sh}} \right)^2 + \frac{5\phi^2}{R_w R_t (1 - V_{sh})}} - \frac{V_{sh}}{R_{sh}} \right\}$$

Calculation of S_w using this equation, an R_w assumption of .15 and using the same sets of data we used for the Archie Equation yield lower water saturations. The distribution of this data is illustrated in Figure 9. The combination of the excellent Company B density data with the Company A resistivity data gives us a believable S_w distribution with few water saturations over 100% or less than 25%. The combination of Company B density porosity with Company B resistivity data yields unrealistically high water saturations, telling us either that our R_w assumption is too high, or that Company B resistivity reads too low.

How can we resolve these interpretation problems? How can we obtain realistic water saturation calculations irrespective of faulty R_t measurements or poor R_w assumptions? One technique is the crossplot.

Resistivity-porosity crossplots are discussed by Pickett (1966) and Lang (1972). They have had numerous applications in the evaluation of thick sand-shale sequences where some of the sands contain 100% water and R_w remains relatively constant throughout the interval. Their use requires good porosity data and interpretation, and in general, they are more satisfactory when there is a normal distribution of high and low porosity sand beds.

Application of the R_t - ϕ crossplot in the Mesaverde can be used to assess log quality. In the event that valid porosity data exists, it can be also used to normalize the resistivity data.

Figure 5 is a crossplot of Company B data. Logarithm of resistivity is plotted on the ordinate vs. logarithm of density porosity on the abscissa. The distribution of Mesaverde Sands ideally defines a straight line of 100% water saturation. Points tend to lie statistically about either side of this line. The line is inclined on a slope "m" which is the "cementation exponent" in the Archie Equation. The intersection of this line with the line of 100% porosity yields the value of "aR_w," which is the "a" coefficient in the Archie Equation multiplied by the formation water resistivity. In this example, the line has a slope of 2.14 and an intersection point at .052.

Great care must be exercised in selecting zones for the crossplot. Subtle variation in porosity or resistivity must be noted and carefully correlated. An example of how we subdivided various zones is indicated along the left margin of Figure 4. Porosity values as low as 4% must be included in order to allow a sufficiently broad range for line construction. Porosities less than 4% proved unsatisfactory because of lower than expected resistivities. There was an attempt to exclude very shaly sands and those that were less than 3 feet thick. Peak values were read for resistivity and statistically averaged values for density porosity.

A crossplot of all Company A data is presented in Figure 6. This plot fails to define an adequate line of 100% water saturation. We interpret this as meaning that the Company A density porosities are reading generally too high, are inconsistent in lower intervals as compared to uphole logged intervals, and are logged at too fast a rate for bed definition of thin sands.

Figure 7 further substantiates these conclusions. This crossplot plots Company A resistivity vs. Company B porosity. An excellent line of 100% water saturation is established. The "m" is 2.07 and "aR_w" is .083. The Company B density porosity serves well to define the 100% water saturation line with either set of resistivity data. The Company A density porosity fails to establish this line and is discarded as poor data.

Using the information gained from these crossplots, the Archie Equation becomes for CIGE 21 Mesaverde Company B data:

Equation 5:

$$S_w^n = \frac{.052}{\phi^{2.14} R_t}$$

The Archie Equation becomes:

Equation 6:

$$S_w^n = \frac{.083}{\phi^{2.07} R_t}$$

for Company A resistivity data and Company B density porosity. For lack of better information saturation exponent "n" is assumed to be 2. Figure 10 compares the above-mentioned sets of data. Both histograms yield somewhat high but ballpark water saturation distributions. The important point is that very similar water saturations are calculated using either set of resistivity data. The crossplots have essentially normalized differences in resistivity. This is especially obvious when Figure 10 is compared to Figure 8.

The crossplot information may also be used to revise the Total Shale Relation. Equation 3 is expressed in its general form:

Equation 7:

$$\frac{1}{R_t} = \frac{\phi_w^m S_w^n}{a R_w (1 - V_{sh})} + \frac{V_{sh} S_w}{R_{sh}}$$

which through quadratic solution becomes:

Equation 8:

$$S_w = \frac{a R_w (1 - V_{sh})}{2 \phi_w^m} \left\{ \sqrt{\left(\frac{V_{sh}}{R_{sh}} \right)^2 + \frac{4 \phi_w^m}{a R_w R_t (1 - V_{sh})}} - \frac{V_{sh}}{R_{sh}} \right\}$$

when "n" is assumed equal to 2.

The "m" and "aR_w" values are then substituted into Equation 7 for each data set to arrive at water saturation. The distribution of these water saturations in CIGE 21 Mesaverde is illustrated in Figure 11. There is very good agreement between sets of data when compared to Figure 9. We have therefore normalized the resistivity data.

CONCLUSIONS

Through crossplot techniques, and subsequent modification of existing water saturation equations, we have arrived at similar saturations irrespective of high or low resistivity values. Using the expression, "aR_w," we have calculated "S_w" without solving for "a" or "R_w" individually. This is important because "R_w" from produced water is not the same as "R_w" in situ. We have discussed this phenomenon in terms of surface conductivities and cation exchange.

The paper has demonstrated the necessity of obtaining valid porosities in order for " R_t - ϕ " crossplots to yield meaningful values of " aR_w ," or " m ." If errors are consistent throughout the log, it may be possible to normalize porosity using methods outlined by Neinast and Knox (1973). We have outlined techniques to insure better quality control of density measurements.

We are not drawing any conclusions as to whether the equations used in this paper arrive at exact water saturations in the Mesaverde. This will be better evaluated by:

1. Surface conductivity research now being done by Bartlesville Energy Research Center.
2. Clay SEM, x-ray diffraction studies, and cation exchange capacity data being gathered by the USGS.
3. Comprehensive core analysis.
4. Production testing of individual zones before frac.
5. New and innovative log interpretation techniques.

NOMENCLATURE

a	=	Dimensionless constant
aR_w	=	a constant X formation water resistivity
m	=	Cementation exponent
n	=	Saturation exponent
ϕ	=	Effective porosity
ϕ_d	=	Porosity derived from Density log
R_{lld}	=	Resistivity as measured by the deep laterolog
R_{sh}	=	Resistivity of shale component
R_t	=	Formation resistivity
R_w	=	Formation water resistivity
R_{xo}	=	Resistivity of the flushed zone
S_w	=	Water saturation volume percent
V_{sh}	=	Volume percent shale

ACKNOWLEDGEMENTS

The encouragement, support, and suggestions of CER technical staff and management are gratefully acknowledged. Appreciation is also extended to Gas Producing Enterprises for cooperating in the WGSP, and to WGSP Manager, C.H. Atkinson, for his direction in this research.

REFERENCES

- Archie, G.E.: "The Electrical Resistivity Log as an aid in Determining Some Reservoir Characteristics," J. Pet. Tech., January 1942, pp 54-62.
- Asquith, D.O.: "Petroleum Potential of Deeper Lewis and Mesaverde Sandstones in the Red Desert, Washakie and Sand Wash Basins, Wyoming and Colorado," Rocky Mountain Association of Geologists Symposium, 1975.
- Boardman, C.R.; Hammack, G.W.; Fertl, W.H. and Atkinson, C.H.: "Evaluation of Low Permeability Gas-Bearing Formations in Rio Blanco County, Colorado," Presented as Paper SPE 4097, Soc. Pet. Eng. 47th Annual Fall Meeting, October 1972.
- Clavier, C.; Coates, G. and Dumanoir, J.: "The Theoretical and Experimental Bases for the 'Dual Water' Model for the Interpretation of Shaly Sands," Presented as Paper SPE 6859, Pet. Eng. 52nd Annual Fall Technical Conference, October 1977.
- Fertl, W.H. and Hammack, G.W.: "A Comparative Look at Water Saturation Computations in Shaly Pay Sands," Trans. SPWLA 12th Annual Logging Symposium, May 1971, Paper R.
- Lang, W.H., Jr.: "Porosity-Resistivity Cross-Plotting," Trans. SPWLA 13th Annual Logging Symposium, May 1972, Paper F.
- Neasham, J.W.: "The Morphology of Dispersed Clay in Sandstone Reservoirs and Its Effect on Sandstone Shaliness, Pore Space and Fluid Flow Properties," Presented as Paper SPE 6858, Soc. Pet. Eng. 52nd Annual Fall Technical Conference, October 1977.
- Neinast, G.S. and Knox, C.C.: "Normalization of Well Log Data," Trans. SPWLA 14th Annual Logging Symposium, May 1973.
- Patchett, J.G.: "Log Interpretation of the Tertiary and Upper Cretaceous of Wyoming and Surrounding Areas," Wyoming Geological Association Guidebook, 16th Annual Field Conference, 1961.
- Pickett, G.R.: "A Review of Current Techniques for Determination of Water Saturation From Logs," J. Pet. Tech., November 1966, pp 1425-1433.

Ratliff, J.R.; Throop, W.H.; Williams, F.G. and Hall, J.D.: "Applications of the SARABAND Sand-Shale Technique in North America," Paper by Schlumberger Services.

Rieke, H.H. and Chilingarian, G.V.: "Compaction of Argillaceous Sediments," Developments in Sedimentology 16, Elsevier Scientific Publishing Company, 1974.

Schufle, J.A.; Huang, C. and Drost-Hansen, W.: "Temperature Dependence of Surface Conductance and a Model of Vicinal (Interfacial) Water," Journal of Colloid and Interface Sciences, Vol. 54, No. 2, February 1976, pp 181.

Short, J.A.: "Massive Frac Treatments Tapping Tight Gas Sands in Uinta Basin," Oil and Gas Journal, January 1978, pp 71-77.

Waxman, M.H. and Smits, L.J.M.: "Electrical Conductivities in Oil-Bearing Shaly Sands," Trans. Soc. Pet. Eng. 42nd Annual Fall Meeting, October 1967.

Weaver, C.E.: "Clay Minerology of the Late Cretaceous Rocks of the Washakie Basin," Wyoming Geological Association Guidebook, 16th Annual Field Conference, 1961.

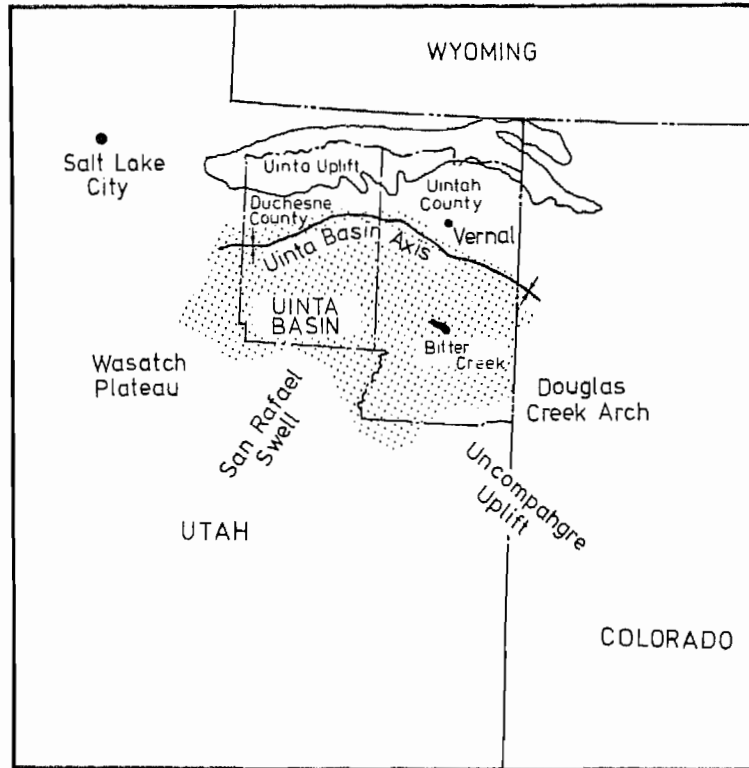


FIGURE 1 UINTA BASIN, UTAH

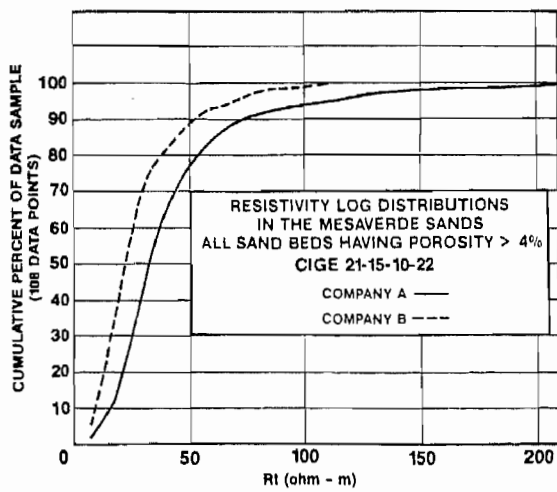


FIGURE 2

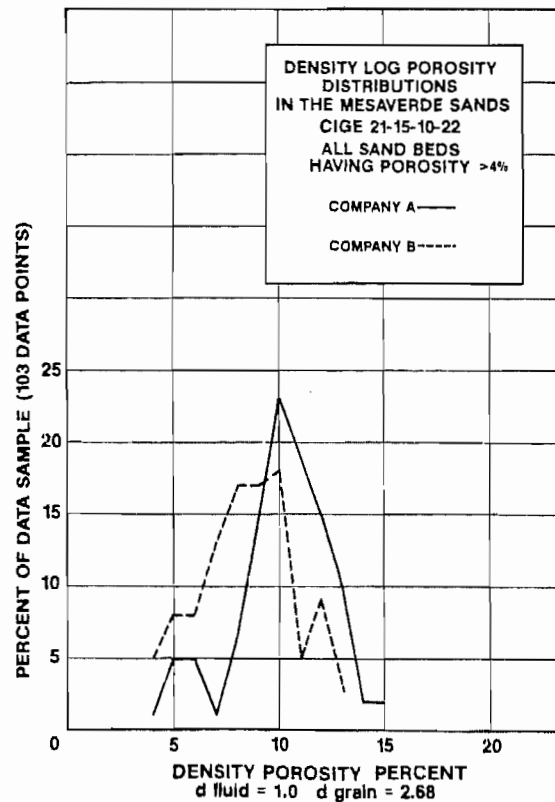


FIGURE 3

TYPE MESAVERDE COMPOSITE LOG CIGE 21-15-10-22

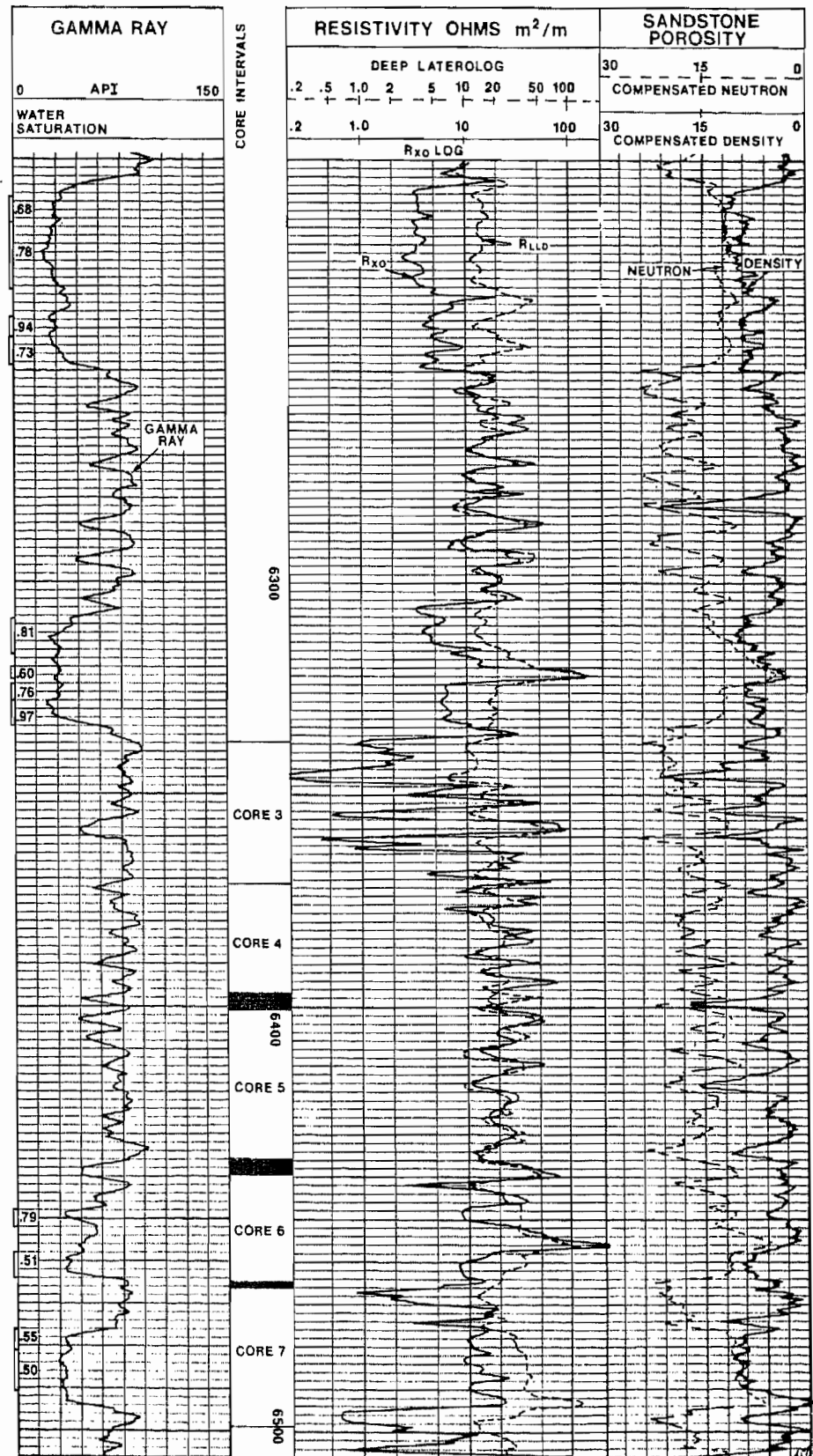


FIGURE 4

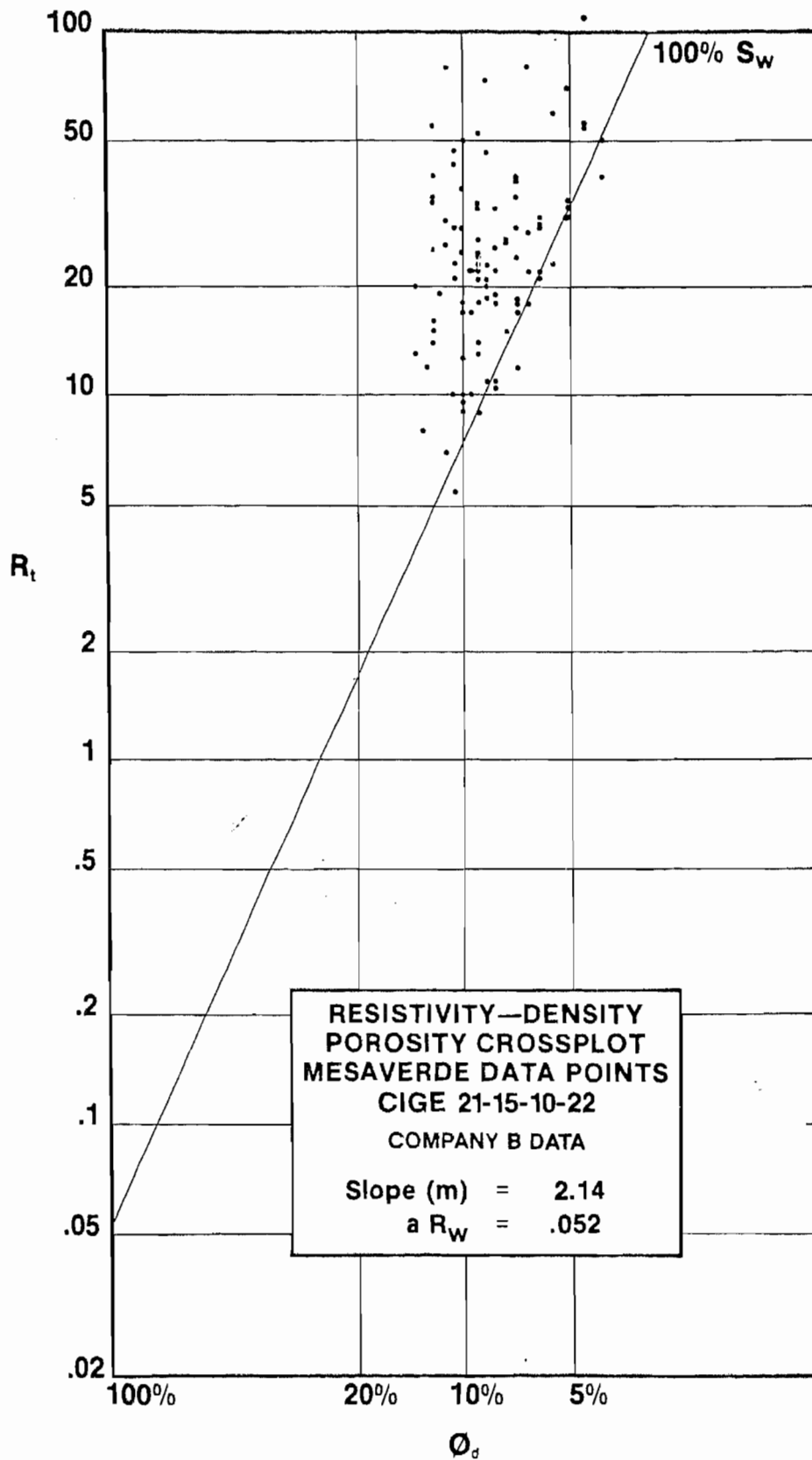


FIGURE 5

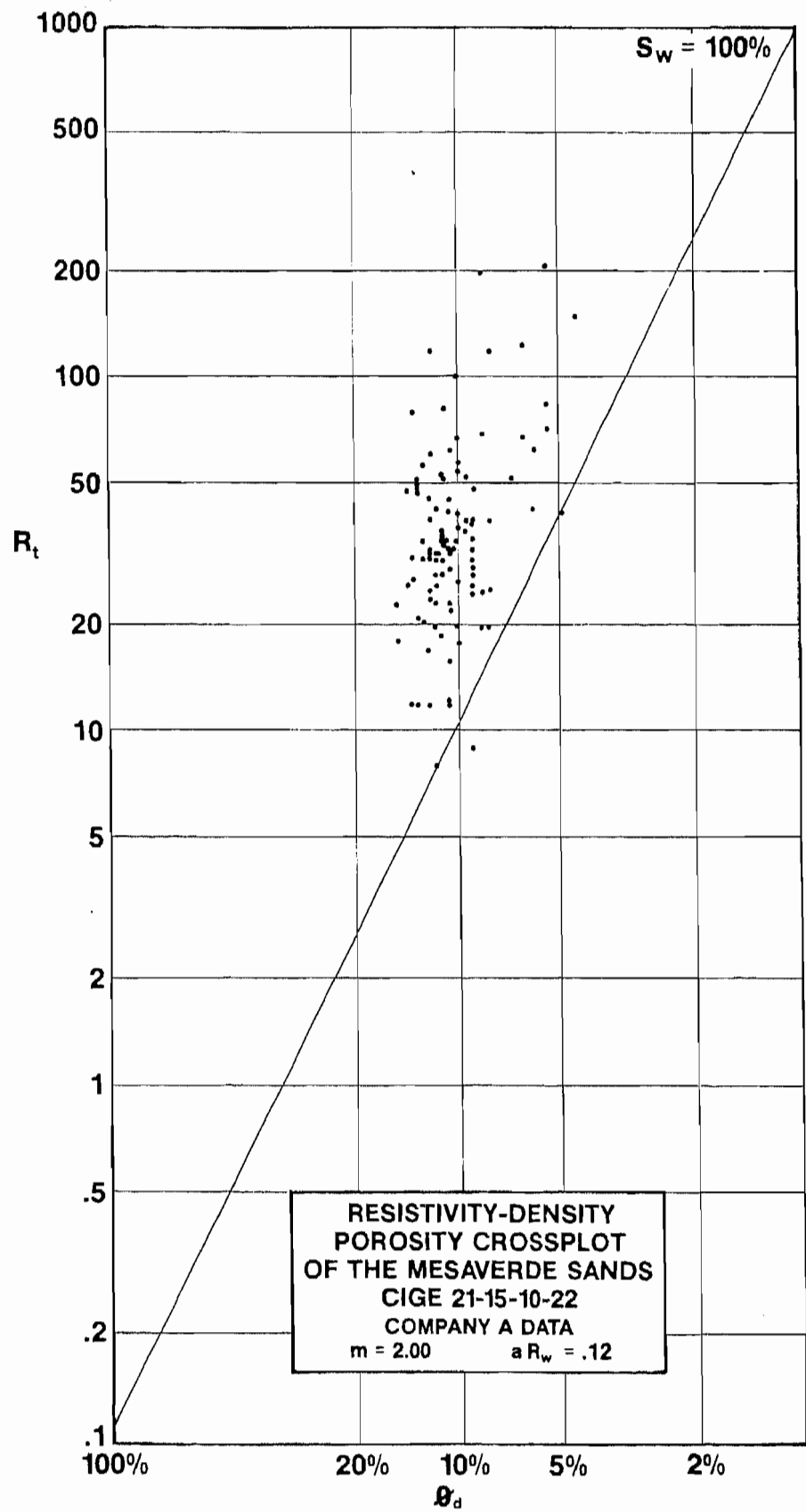


FIGURE 6

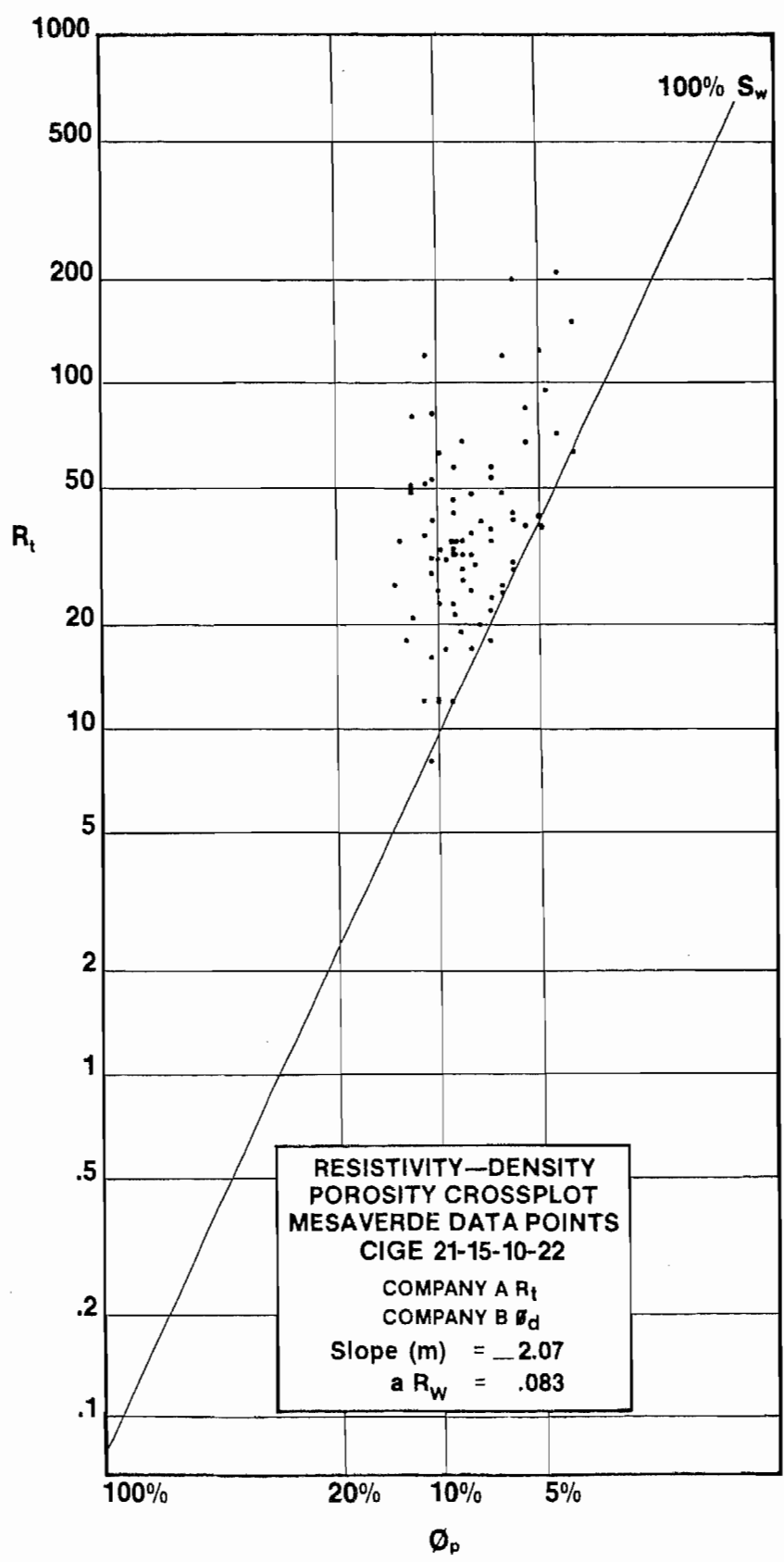


FIGURE 7

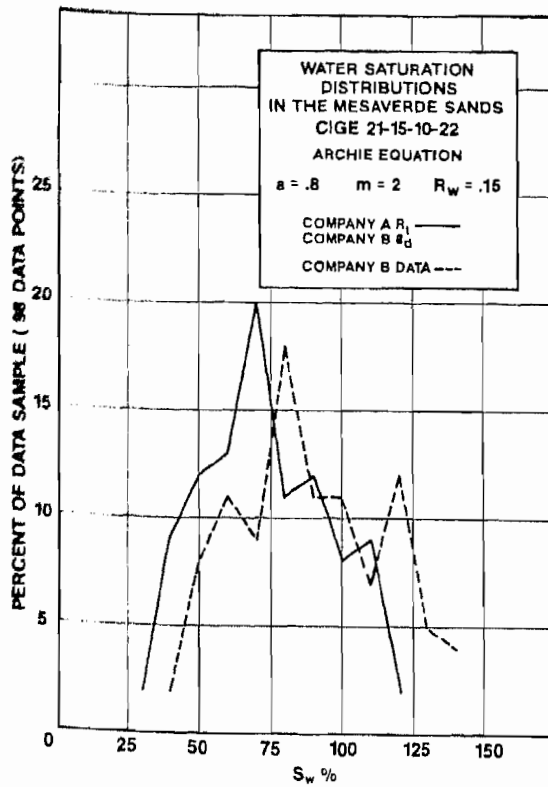


FIGURE 8

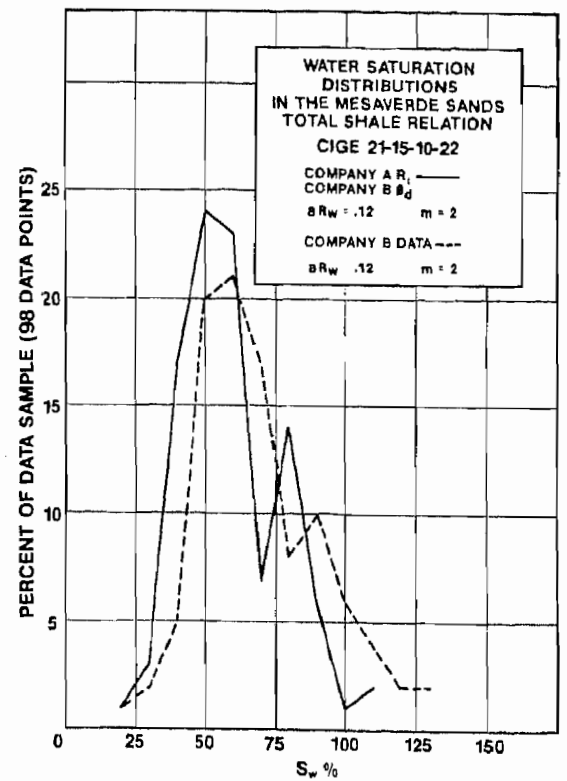


FIGURE 9

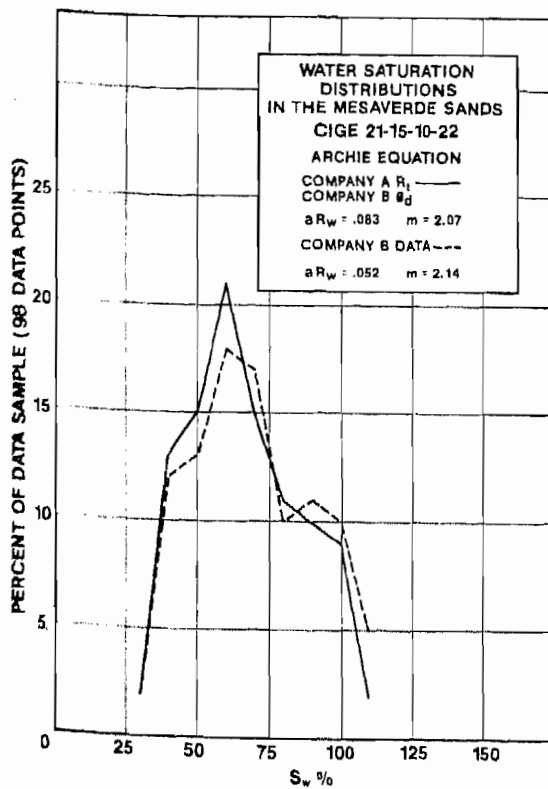


FIGURE 10

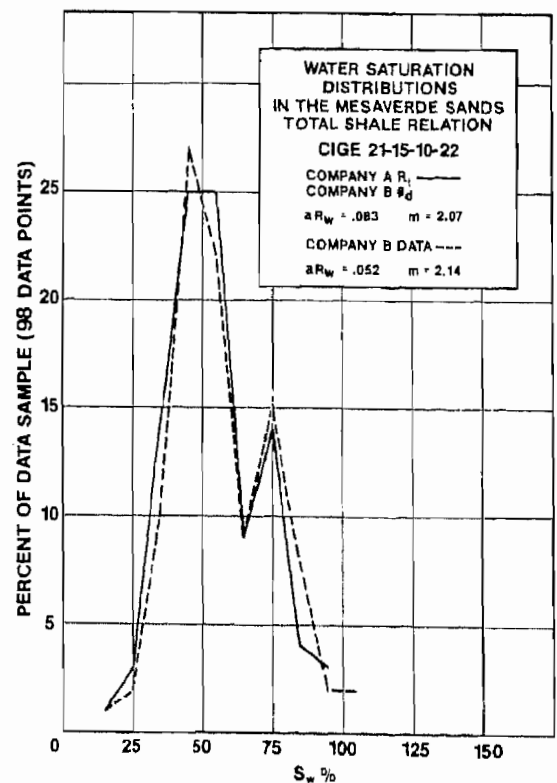


FIGURE 11